Numerical simulations of rough contacts between viscoelastic materials

S Spinu[1,2*] **and D Cerlinca**[1,2]
[1] Department of Mechanics and Technologies, Stefan cel Mare University of Suceava, 13th University Street, 720229, Romania
[2] Integrated Center for Research, Development and Innovation in Advanced Materials, Nanotechnologies, and Distributed Systems for Fabrication and Control (MANSiD), Stefan cel Mare University, Suceava, Romania

E-mail: sergiu.spinu@fim.usv.ro

Abstract. The durability of the mechanical contact is often plagued by surface-related phenomena like rolling contact fatigue, wear or crack propagation, which are linked to the important gradients of stress arising in the contacting bodies due to interaction at the asperity level. The semi-analytical computational approach adopted in this paper is based on a previously reported algorithm capable of simulating the contact between bodies with arbitrary limiting surfaces and viscoelastic behaviour, which is enhanced and adapted for the contact of real surfaces with microtopography. As steep slopes at the asperity level inevitably lead to localized plastic deformation at the tip of the asperities that are first brought into contact, the viscoelastic behaviour is amended by limiting the maximum value of the pressure on the contact area to that of the material hardness, according to the Tabor equation. In this manner, plasticity is considered in a simplified manner that assures the knowledge of the contact area and of the pressure distribution without estimation of the residual state. The main advantage of this approach is the preservation of the algorithmic complexity, allowing the simulation of very fine meshes capable of capturing particular features of the investigated contacting surface. The newly advanced model is expected to predict the contact specifics of rough surfaces as resulting from various manufacturing processes, thus assisting the design of durable machine elements using elastomers or rubbers.

1. Introduction

The assessment of the contact area, contact tractions and surface deformation arising in the mechanical contact of solids bounded by rough surfaces is a fundamental problem in Contact Mechanics, whose importance stems from the fact that various modes of wear (surface-initiated rolling contact fatigue, fatigue wear or sliding wear) are driven by microtopography-induced stress perturbations. When two machine elements are brought into contact and load is transmitted, interfacial tractions occur due to direct interaction of the two surfaces at the asperity level, generating a discrete contact area defined as the set of individual contact spots. The knowledge of this contact area and of the associated gap between the contacting surfaces may be crucial in assessing the thermal or electrical conductivity of the contact, as well as its sealing capacity. At this moment, the only approach that can account for microcontact interaction is the direct numerical resolution of the contact problem with real specimens of roughness as measured with 3D surface imaging devices, or with computer generated surfaces.

Content from this work may be used under the terms of the Creative Commons Attribution 3.0 licence. Any further distribution of this work must maintain attribution to the author(s) and the title of the work, journal citation and DOI.
Published under licence by IOP Publishing Ltd

Various domains of the engineering use composite materials that are based on viscoelastic matrix. The structural complexity of these materials prohibits the development of mathematical models that are solvable within the framework of contact mechanics. Most of the existing solutions are limited to specific contact geometries and ideal models of viscoelastic behavior with only one relaxation time. The solution of the Hertz contact problem was firstly obtained by Lee and Radok [1] for linear viscoelastic materials, under the assumption of a monotonically increasing contact area. This assumption was later released by Ting [2,3], who advanced an implicit solution for the contact of axisymmetric bodies generating a contact area described by an arbitrary function of time.

The semi-analytical treatment of the viscoelastic contact problem was pioneered by the work of Chen et al. [4]. The main advantage of the semi-analytical approach consists in the release of the assumptions concerning the contact geometry, the loading history or the constitutive law of the viscoelastic material. A previously proposed algorithm [5] for the linear viscoelastic contact of bodies of arbitrary boundaries is enhanced and adapted to simulate the contact of rough surfaces with steep asperities acting as pressure concentrators.

2. Assumptions and limitations

The assumptions needed for the solution of the rough contact problem involving linear viscoelastic materials fall into two categories: (1) the contact model assumptions, (2) and the ones related to the mechanical response of the viscoelastic material, i.e. the constitutive law.

The contact model employed in this paper features the classical assumptions [6] needed to solve the contact problem in an iterative manner. The half-space approximation is employed in computation of surface displacement, empowering the use of the Boussinesq fundamental solution for a point force acting normally on the boundary of an elastic half-space. Consequently, bodies of arbitrary surface profiles are assumed as semi-infinite linear elastic solids bounded by a plane surface, which is reasonable in case of infinitesimal strains arising in concentrated contacts, when the contact area is small compared to the dimensions of the contacting bodies. Friction is neglected for brevity, meaning the contact interface cannot sustain shear tractions. As shown in [7], while there is no conceptual difficulty in incorporation of friction in a slip-stick contact model, the additional iterative loop needed to stabilize the mutually dependent contact problems in the normal and in the tangential direction is very computationally intensive. Moreover, the normal contact tractions are assumed to be compressive only. In the framework proposed in this paper, the contact solution is achieved using an optimization scheme which requires the non-negativity of contact tractions. The contact process was modeled as a variational problem by these authors [8], in which the desired pressure distribution achieves the minimum of a quadratic form, i.e. the complementary energy, subjected to constraints, i.e. the boundary conditions. The convergence of this quadratic optimization is guaranteed for compressive tractions (pressure) only. It should be noted that adhesion was not accounted for either in the classic or the modern literature [1-4] of the viscoelastic contact. The viscoelastic solution advanced in [2] employs a displacement field matching closely the indenter profile within the boundaries of the contact area, but does not guarantee that contact tractions are everywhere compressive. As shown in [9], the incorporation of adhesion in a contact model leads to equations that are highly nonlinear and may have multiple singularities, requiring the use of special numerical techniques such as the Particle Swarm Optimization method.

On the other hand, simplifying assumptions are needed for the constitutive law of the viscoelastic material as well. Computational contact mechanics can incorporate the theory of viscoelastic behavior provided a directly additive (i.e., linear) viscoelastic response is assumed, which is reasonable in the framework of infinitesimal strains. This assumption of linearity provides the basis for the mathematical modeling of viscoelasticity, allowing for the computation of responses to arbitrary sequences of stress or strain within the Boltzmann superposition theory. In this framework, the viscoelastic material response to various sequences of stress or strain can be assessed according to the Boltzmann hereditary integral, by employing two interchangeable functions of time, namely the relaxation modulus $\Psi(t)$ and the creep compliance $\Phi(t)$. The creep compliance function describes

the viscoelastic strain response to a unit step change in stress, and the relaxation modulus, conversely, the stress response to a unit step change in strain.

As opposed to nominal (or theoretical) contact shapes, the contact of real surfaces occurs at discrete spots due to inherent surface roughness. As the initial contacting asperities tips become flattened, lower asperities come into contact, leading to an increasing contact area that can sustain the applied load. It is reasonable to assume that even at low loading levels, plastic deformation may occur at the asperities tips, especially when the slope of the single asperity is high. In the discrete numerical model, this slope may be exaggerated by a coarse mesh, in which only one grid is available for the asperity tip.

Many research efforts were dedicated to the integration of plasticity in the contact model. The first complete formulation of an elastic-plastic contact model and its associated computer code, featuring three nested iterative levels, was reported by these authors [10]. Subsequent iterations of the latter improved on the convergence of the inner residual loop, while extending the generality of the plasticity hardening law. Essentially, the elastic-plastic contact problem is divided into an elastic and a residual subproblem, which are mutually dependent. The elastic subproblem bare resemblances with contact solver employed in this paper, while the residual part is based on a universal algorithm [11] for integration of elastoplasticity equations and on the numerical solution of the inclusion problem [12]. Both viscoelastic and elastic-plastic contact problems are history dependent and therefore require path discretization. Extension of the elastic-plastic strategy to viscoplastic materials is tantalizing, an important step being made by these authors [13], who extended the solution of the inclusion problem to viscoelastic materials, by applying the Eshelby's formalism [14] to an ellipsoidal inhomogeneity located in a viscoelastic matrix. Based on the solution of the inclusion problem with an elastic matrix [15], the computation of the residual part in viscoplastic materials is expected to have a great impact on the algorithmic complexity, due to extension of the surface discretization inside the viscoplastic material. Therefore, the development of a fully-fledged contact model incorporating both viscoelasticy and plasticity is beyond the scope of this paper.

In the contact model employed in this paper, plasticity is accounted for in a simplified manner that preserves the spatial discretization requirements to two dimensions. It should be noted that a similar assumption, that of imposing a cut-off value to contact pressure, has been employed in many works on the elastic-plastic contact of rough surfaces, as discussed in the next section.

3. Contact model and algorithm overview

The contact model employed in this paper is an extended version of a previous work by the same authors [5]. It features a 2D spatial discretization, allowing for iteration of contact area and of pressure distribution, as well as a temporal discretization, required for reproduction of the memory effect specific to viscoelastic materials. Consequently, the model parameters are functions of at most three arguments, the first two being reserved for spatial and the third one for temporal localization. The problem model is repeated for clarity, and new constraints are added:

$$W(k) = \Delta \sum_{(i,j)\in A(k)} p(i,j,k), \quad k = 1 \ldots N_t; \tag{1}$$

$$h(i,j,k) = hi(i,j) + u(i,j,k) - \omega(k), \quad (i,j) \in P, k = 1 \ldots N_t; \tag{2}$$

$$p(i,j,k) > 0 \quad \text{and} \quad h(i,j,k) = 0, \quad (i,j) \in P, k = 1 \ldots N_t; \tag{3}$$

$$p(i,j,k) = 0 \quad \text{and} \quad h(i,j,k) > 0, \quad (i,j) \in P - A, k = 1 \ldots N_t; \tag{4}$$

$$u(i,j,k) = \sum_{n=2}^{N_t} \sum_{\ell=1}^{N_1} \sum_{m=1}^{N_2} K(i-\ell, j-m, k-n)\big(p(\ell,m,n) - p(\ell,m,n-1)\big), \ (i,j) \in P, k = 2 \ldots N_t; \tag{5}$$

$$p(i,j,k) < H, \quad (i,j) \in P, k = 1 \ldots N_t . \tag{6}$$

Here, W denotes the applied normal force, A the set of elementary cells best fitting the shape of the contact area, P the computational domain, p the contact pressure, hi the gap between the undeformed surfaces at time $t = 0$, N_1 and N_2 the number of grids in the spatial discretization, N_t the number of temporal steps, h the gap between the deformed surfaces, u the relative normal displacement, ω the rigid-body approach, H the hardness of the softer material, and $K(i-\ell, j-m, k-n)$ the viscoelastic influence coefficient, expressing the displacement induced in the (i,j) patch of the spatial mesh after k time steps, by a unity uniform pressure that acted in the patch (ℓ, m) after n time steps, with $n \le k$.

A robust algorithm for the contact model consisting in the set of equations (1) - (5) was previously advanced by these authors [5]. When applied to rough contact problems with steep slopes on the contact area, the latter model, while conceptually sound, predicts highly isolated pressure peaks related to the tips of the asperities that first come into contact. It is highly unlikely that the entire load can be sustained by a few asperities only. In reality, these higher asperities will deform plastically and become flattened, bringing additional lower asperities into contact, resulting in an enlarged contact area that can accommodate the applied load. It is in this later stage of the contact process that a purely viscoelastic response can be assumed for the contacting materials.

Consequently, in order to apply the contact model (1) - (5) to viscoelastic rough surfaces, the matter of unrealistic pressure peaks has to be addressed. In dealing with this inadequacy, many authors [16, 17] have employed the Tabor equation [18] in the study of the elastic-plastic contact of rough surfaces. This equation basically establishes the relation between the local normal strength p_m, the local shear strength τ_m and the hardness H of the softer material in the form:

$$p_m^2 + \alpha \tau_m^2 = H^2 , \tag{7}$$

where α is the Tabor constant, generally determined from experimental measurements. For elastic – perfectly-plastic materials, H≈2.8σ_Y, where σ_Y is the uniaxial yield strength. As in our model the contact interface cannot sustain shear tractions, $\tau_m = 0$, and consequently the hardness of the softer material can be used as a cut-off value for the local pressure, as resulting from equation (7). Consequently, the model for the contact of linear viscoelastic materials bounded by rough surfaces is completed with the equation (6), which adds supplementary boundary conditions to the initial model. The algorithm previously proposed for the contact model (1) - (5) can be adapted to account for the supplementary constraint (6) imposed to the contact pressure. The required modifications are discussed here.

The algorithm aims to solve the linear system of equations resulted from equation (2), having the nodal pressures as unknowns. This is accomplished by employing the Conjugate Gradient Method (CGM), due to its superlinear rate of convergence. However, in the initial formulation [5] for the set (1) - (5), only cells with positive pressures were considered in the computation of the parameters required by the CGM: the residual, the descent direction, the length of the step to be made along the descent direction. In other words, not every combination of the indices (i,j) from relation (2) generates equations that are useful to compute the pressure distribution. By adding or substracting equations from the linear system, based on the complementarity conditions (3) and (4), the contact area itself is adjusted with each new iteration.

The negativity of a nodal pressure was used in the original algorithm as a criterion for excluding the corresponding cell from the contact area and the corresponding equation from the linear system. Once extracted from the contact area, the cell is assigned a vanishing nodal pressure. In the same manner, equations of the form (2) corresponding to cells (i,j) with pressures that exceed the material hardness are excluded from the system resolution process (i.e. from the computation of the residual, of

the descent direction and of the descent step). To these cells, a pressure equal to the material hardness is assigned.

The performed numerical simulations suggest that the algorithm speed of convergence is not affected by the modifications required to accommodate the supplementary boundary condition (6). This simplified manner of imposing a plasticity related correction to the viscoelastic model, while not being able to predict the residual state resulting from the plastic flow process, allows for the computation of the pressure distribution and of the contact area with only a two-dimensional spatial mesh. In this manner, the computational resources can be used for the accurate capturing of rough surface specific features by using finer meshes. It should be noted that, whereas the simulation of an elastic-plastic contact process is usually performed on a grid with 64^2 points on the contact area, the roughness sample used in this paper has 512^2 individual heights.

4. Numerical simulations and results

To better clarify the effect of the additional constraints imposed on the pressure distribution, a single asperity spherical contact was simulated in the elastic domain. The Hertz contact parameters, namely the central maximum pressure p_H and the contact radius a_H, were used as normalizers in figure 1, depicting the pressure profiles in a radial plane. The normal load was chosen so that the maximum pressure exceeds the hardness of the material. In the purely elastic simulation (i.e. without the additional constraint (6)), the pressure is semi-ellipsoidal, in accord with the Hertz solution. When the limiting of the pressure is imposed, the numerically predicted contact area keeps its circular aspect, but a central circular plateau appears at the level of the cut-off limit imposed for the contact pressure. In order to compensate for the conventional limiting of pressure and to sustain the applied load, the contact radius increases, as resulting from figure 1.

In a fully-fledged elastic-plastic contact code, with full computation of the residual state, the increase of the contact area with the development of plastic strains inside the elastic material is the result of modification in contact conformity due to residual displacement. The grid that can be solved with the elastic-plastic code [10] is considerably coarser than the one used in this paper, as the spatial discretization needs to be extended in the third dimension (in depth) to assess the plastic strains developed in the softer material. The simplified manner in which plasticity is accounted for in the model proposed herein promises [16,17] accurate estimation of contact area and of pressure distribution while preserving the computational complexity of the contact solver to that of a purely elastic contact scenario.

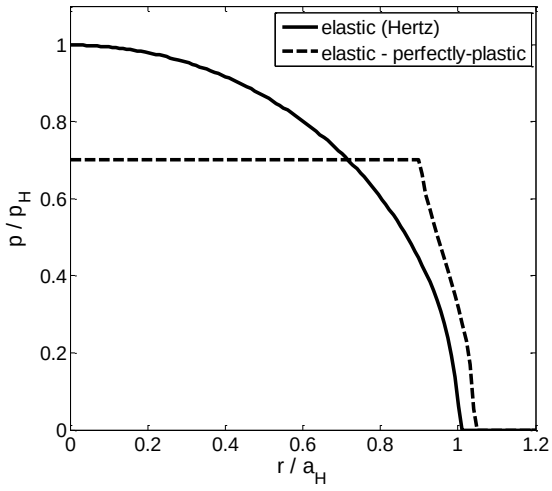

Figure 1. Radial pressure profiles in the spherical contact.

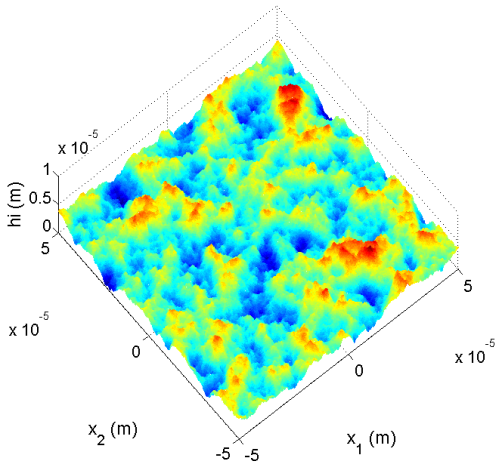

Figure 2. Deterministic roughness sample.

The simulation of the rough viscoelastic contact is performed using a deterministic (i.e. obtained by actual measuring of a real specimen) roughness sample, consisting in the discrete heights of 512×512 equidistant points laying in a rectangular patch of side lengths 0.1×0.1 mm, as shown in figure 2. The points with the lower heights touch the counter surface (a rigid flat) first.

Two contact simulation are firstly performed without considering the effect of viscoelasticity (i.e. at time $t = 0$ s, under the assumption that the body was previously undisturbed), aiming to better clarify the effect of pressure limitation in a rough contact problem involving real microtopography. The contact model without the additional pressure constraint (6) predicts highly isolated pressure peaks related to the asperity tips with steep slopes, as shown in figure 3. Such levels of contact tractions, one order of magnitude greater than the hardness of the material, cannot be sustained without severe plastic deformation. The limiting of pressure, as depicted in figure 4, helps alleviate these spurious pressure concentrators and results in additional contact spots related to lower asperities, thus leading to a presumably more realistic prediction of the contact area. For comparison purposes, the same pressure scale of was used in both figures 3 and 4. It should also be noted that the contact area in figure 4 is roughly 3.2 times the one predicted from the purely elastic computation in figure 3.

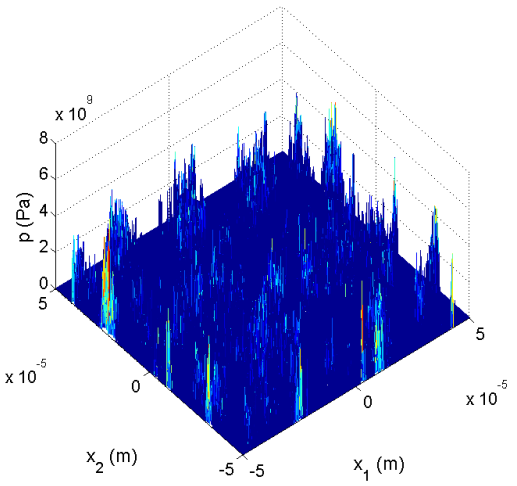

Figure 3. Pressure distribution in rough contact, purely elastic analysis. Maximum nodal pressure $p_{\max} = 6.45$ GPa .

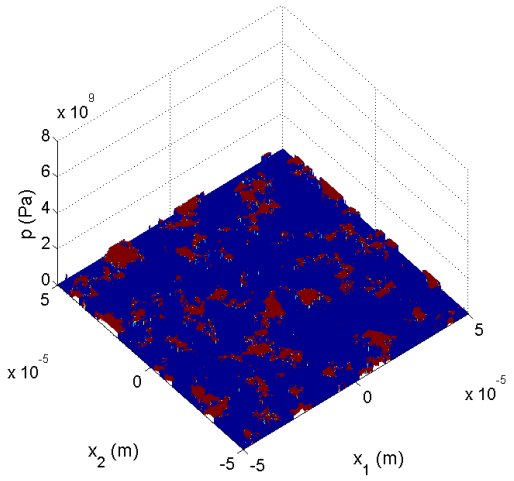

Figure 4. Pressure distribution with consideration of plasticity. Maximum nodal pressure $p_{\max} = H = 300$ MPa .

The considered constitutive law for the viscoelastic material is that of the polymethyl methacrylate (PMMA), a thermoplastic polymer whose mechanical properties were studied extensively by Kumar and Narasimhan [19]. The relaxation modulus of PMMA was measured experimentally up to 1000 s under uniaxial compression. Whereas classical rheological models like the Maxwell or the Kelvin units, having only one relaxation time, are adequate for qualitative description of the viscoelastic behavior, the naturally occurring spectrum of relaxation times of a viscoelastic material can be modeled by a Prony series (corresponding to a Weichert model), by including as many exponential terms as required. The Weichert model consists in several Maxwell units and a free spring, all connected in parallel, having the relaxation modulus:

$$\psi(t) = g_0 + \sum_{i=1}^{n} g_i \exp\left(\frac{-t}{\tau_i}\right), \tag{8}$$

where g_0 is the spring stiffness of the free spring, and τ_i and g_i the relaxation time and the spring stiffness of each Maxwell unit.

A two-term Prony series (i.e. with two relaxation times) was fitted [4] to the experimental data of the PMMA, leading to the following relaxation curve:

$$\psi(t) = 1429.71 + 184.62\exp\left(\frac{-t}{8.93}\right) + 191.06\exp\left(\frac{-t}{117.96}\right), \quad \text{(MPa)}. \tag{9}$$

The hardness of the PMMA was considered as indicated in [19], $H = 300$ MPa. A step loading with $W = 0.5$ N was simulated in a time interval of 1000 s, divided into 200 equal time increments. The contact area maps in the beginning and at the end of the simulation window are presented in figures 5 and 6. Comparison of the two plots shows that the contact area, defined as the sum of all discrete contact spots, grows with time. Additional asperities that were brought into contact at the end of the simulation window due to viscoelasticity effects, are indicated in figure 6 using dashed lines.

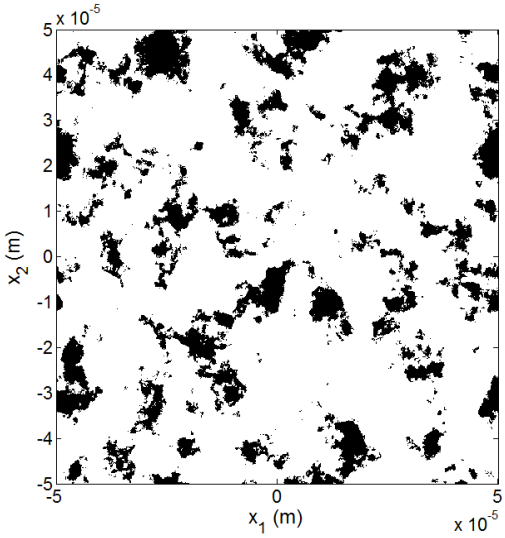

Figure 5. Contact area map at $t = 0$ s.

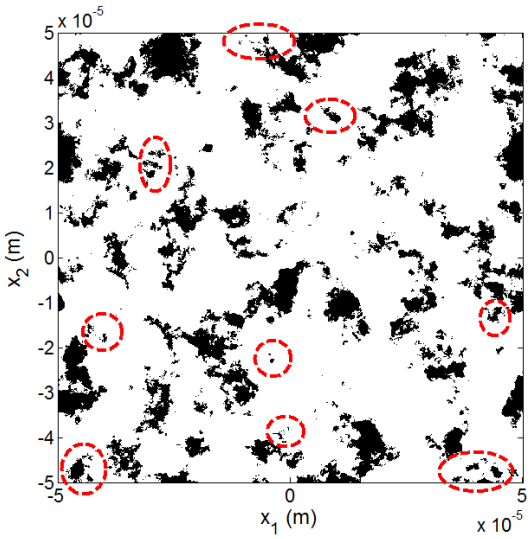

Figure 6. Contact area map at $t = 1000$ s.

The evolution of the contact area with time is presented in figure 7. In the beginning of the simulation window, the creep effect of the viscoelastic material flattens the contacting asperities, bringing lower asperities into contact. As time goes on, the creep process stabilizes due to delayed elasticity and the contact area grows with time more slowly.

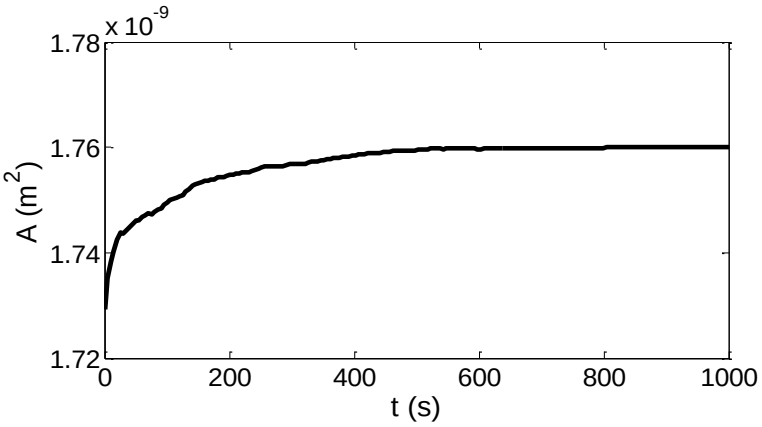

Figure 7. Evolution of the contact area with time.

5. Conclusions

This paper advances the generalization of a previously reported contact code for simulation of contact processes involving viscoelastic bodies of arbitrary surface profile. The generalization consists in imposing additional constraints to the nodal pressure computed exclusively from the geometrical condition of deformation.

It was found that direct application of the algorithm for arbitrary contact geometry, while sound in case of smooth limiting surfaces, leads to highly concentrated pressure peaks when inputting deterministic rough surfaces. While the assumption of a viscoelastic deformation is clearly too conservative for the asperity tips that enter the contact first, the incorporation of plasticity in the viscoelastic contact model lacks mathematical support. Moreover, based on the similitude with the elastic-plastic contact problem, computation of the residual state, requiring the solution of the inclusion problem, is likely to have a huge impact on the algorithm computational efficiency. A reasonable compromise is achieved in this paper, by imposing a material dependent threshold for the contact pressure. With this assumption, the contact pressure is computed by a purely geometrical analysis of the surface of deformation. A similar technique was successfully used by other authors in the study of the elastic-plastic rough contact.

The viscoelastic contact simulation employs a deterministic roughness sample with 512×512 equidistant points measured in a rectangular area of side lengths 0.1×0.1mm, and a viscoelastic constitutive law with a relaxation modulus described by a two-terms Prony series, fitted from experimental data for a polymethyl methacrylate specimen in uniaxial compression. The more pronounced contact area growth in the early stages of the contact simulation can be attributed to the viscoelastic creep, and the subsequent stabilization to delayed elasticity.

Acknowledgement

This work was partially supported from the project “Integrated Center for Research, Development and Innovation in Advanced Materials, Nanotechnologies, and Distributed Systems for Fabrication and Control”, Contract No. 671/09.04.2015, Sectoral Operational Program for Increase of the Economic Competitiveness co-funded from the European Regional Development Fund.

6. References

[1] Lee E H and Radok J R M 1960 *ASME J. Appl. Mech.* **27** 438
[2] Ting T C T 1966 *ASME J. Appl. Mech.* **33** 845
[3] Ting T C T 1968 *ASME J. Appl. Mech.* **35** 248
[4] Chen W W, Wang Q J, Huan Z and Luo X 2008 *ASME J. Tribol.* **133** 041404
[5] Spinu S and Cerlinca D 2016 *IOP Conf. Ser.: Mater. Sci. Eng.* **145** 042034
[6] Johnson K L 1985 *Contact Mechanics* (Cambridge: University Press)
[7] Spinu S and Glovnea M 2012 *J. Balk. Tribol. Assoc.* **18** 195
[8] Kalker J J and van Randen Y A 1972 *J. Eng. Math.* **6** 193
[9] Yu H, Li Z, and Wang Q J 2013 *Mech. Mater.* **60** 55
[10] Jacq C, Nelias D, Lormand G and Girodin D 2002 *ASME J. Tribol.* **124** 653
[11] Fotiu P A and Nemat-Nasser S 1996 *Comput. Struct.* **59** 1173
[12] Mura T 1988 *Appl. Mech. Rev.* **41** 15
[13] Kuomi K E, Nelias D, Chaise T and Duval A 2014 *Mech. Mater.* **77** 28
[14] Eshelby J D 1959 *Proc. R. Soc. London, Ser. A* **252** 561.
[15] Spinu S 2013 *Mechanika* **19** 252
[16] Liu S B and Wang Q 2001 *ASME J. Tribol.* **123** 17
[17] Peng W and Bhushan B 2002 *ASME J. Tribol.* **124** 46
[18] Tabor D 1959 *Proc. R. Soc. London, Ser. A* **251** 378
[19] Kumar M V R and Narasimhan R 2004 Curr. Sci. **87** 1088